A COMPRESSED SENSING APPROACH FOR BIOLOGICAL MICROSCOPIC IMAGE PROCESSING

Marcio M. Marim[1,2], Elsa D. Angelini[2], J.-C. Olivo-Marin[1]

[1]Institut Pasteur, Unité d'Analyse d'Images Quantitative CNRS URA 2582, F-75015 Paris
[2]Institut TELECOM, TELECOM ParisTech CNRS LTCI, F-75013 Paris

ABSTRACT

In fluorescence microscopy the noise level and the photobleaching are cross-dependent problems since reducing exposure time to reduce photobleaching degrades image quality while increasing noise level. These two problems cannot be solved independently as a post-processing task, hence the most important contribution in this work is to a-priori denoise and reduce photobleaching simultaneously by using the *Compressed Sensing* framework (CS). In this paper, we propose a CS-based denoising framework, based on statistical properties of the CS optimality, noise reconstruction characteristics and signal modeling applied to microscopy images with low signal-to-noise ratio (SNR). Our approach has several advantages over traditional denoising methods, since it can under-sample, recover and denoise images simultaneously. We demonstrate with simulated and practical experiments on fluorescence image data that thanks to CS denoising we can obtain images with similar or increased SNR while still being able to reduce exposition times.

Index Terms— Compressed Sensing, denoising, multi-scale, biological microscopy, photobleaching

1. INTRODUCTION

In this paper we propose an application of *Compressed Sensing* on fluorescence microscopic images, as a powerful denoising method, enabling the reduction of photobleaching on images under reduced exposition times. Our denoising framework is based on the property of CS to efficiently reconstruct sparse signals with under-sampled acquisition rates, significantly below the Shannon/Nyquist theoretical bound. Similarly to recent experiments for MRI CS-based reconstruction [1], the acquisition protocol consists in measuring the image signal onto a random set of Fourier vectors [2], which is incoherent to the domain where the image is sparse. Indeed, the CS framework introduced by Candès [3] provides theoretical results and shows that if a signal is sparse (i.e. has a small number of non-zero coefficients) in some basis, then with high probability, uniform random projections of this signal onto an unstructured domain, where the signal is not sparse, contains enough information to optimally reconstruct this signal [3]. The incoherence property between the sparsity basis Ψ and the sampling basis Φ ensures that signals having sparse representations in Ψ must have a large support in the measurement domain described by Φ [4]. Random selections of basis

functions in Φ are typically suitable since random vectors are, with very high probability, incoherent with any sparsity-encoding basis functions from Ψ, defining orthogonal domains [5].

In fluorescence microscopy, cellular components of interest in specimens such as proteins are typically labeled with a fluorescent molecule called a fluorophore such as green fluorescent protein (GFP) and can therefore be imaged with high specificity. Fluorophores lose their ability to fluoresce as they are illuminated through a process called photobleaching [6, 7]. In microscopy, observation of fluorescent molecules is challenged by the photobleaching, as these molecules are slowly destroyed by the light exposure necessary to stimulate them into fluorescence. Loss of emission activity caused by photobleaching can be controlled by reducing the intensity or time-span of light exposure. At the same time, reducing the exposure time or intensity of the excitation also reduces the emission intensity but not the noisy acquisition components, leading to a decrease of the SNR. We propose to use the CS sampling and reconstruction framework to denoise and improve the SNR of microscopic fluorescence images acquired with shorter exposure times to reduce photobleaching.

2. METHODS

2.1. Reconstruction from noisy measurements

Considering that a signal x has a sparse representation in some basis Ψ, we want to recover the signal $x \in \mathbb{R}^N$ from noisy measurements $y = \Phi(x + n) \mid y \in \mathbb{R}^M$, the sampling matrix being defined by M vectors in Φ, with $M \ll N$. The presence of noise in the acquired signal might alter its sparsity in the domain Ψ. By optimally reconstructing a signal with explicit sparsity constraints, CS offers a theoretical framework to remove non-sparse random noise components from a corrupted signal. Indeed, removing noise from $x + n$ will rely on the efficacy of Ψ on representing the signal x sparsely and the inefficacy on representing the noise n [8]. The choice of the basis function Ψ is very important and depends directly on the kind of signal (or image) we want to recover and denoise using CS. If we make the assumption that the noise energy is bounded by a known constant $\| n \|_{\ell_2} \leq \epsilon$, the transformed signal Ψx is sparse, and $\Phi \in \mathbb{R}^{MN}$ is a random matrix sampling x in the Fourier domain, the spatial signal x can be recovered nearly exactly using the following convex optimization:

$$\hat{x} = \arg \min_{x \in \mathbb{R}^N} \| \Psi x \|_{\ell_1} \text{ s.t. } \| y - \Phi x \|_{\ell_2} \leq \delta \qquad (1)$$

for some small $\delta > \epsilon$, where the operator Ψ is equivalent to compute the gradient, and hence the ℓ_1 norm of Ψx corresponds to the *Total Variation* (TV) of x, $\| \Psi x \|_{\ell_1} \Leftrightarrow \| \nabla x \|_{\ell_1} = \| x \|_{TV}$. In [9] it

was shown that the solution $\hat{x}$ is guaranteed to be within $C\delta$ ($C \in \mathbb{R}^+$) of the original signal x.

$$\| \hat{x} - x \|_{\ell_2} \leq C\delta \quad (2)$$

We note here that this CS-based estimation framework, with noisy observations and TV spatial constraints [10], guarantees that no false component of $x + n$ with significant energy is created as it minimizes the ℓ_1 norm of $\hat{x}$, which is particularly high for the additive random noise components. More specifically, the TV-based spatial sparsity constraint, will lead to sharp edges and removal of noise components, resulting in an error:

$$\| \hat{x} - x \|_{\ell_2} \leq \alpha + \beta \quad (3)$$

where α reflects the desired error (responsible for noise removal) from the relaxation of the constrain δ in (1) and β reflects the undesired error from Fourier undersampling of the signal. If TV represents x efficiently and n inefficiently, the term β vanishes and $\alpha \to C\delta$.

In the context of microscopic images, noise models usually combine Poisson and Gaussian components, and the observation model commonly adopted is the following:

$$\begin{aligned} I(x,y) = & \; \zeta U_i(A(x,y) + \lambda_B) + V_i, \\ & U_i \sim \mathcal{P}(\lambda_i), \quad V_i \sim \mathcal{N}(\mu, \sigma^2) \end{aligned} \quad (4)$$

where ζ is the overall gain of the detector, $A(x,y)$ is the object intensity, λ_B is the mean intensity of the background, U_i is a Poisson variable modeling the photon counting and V_i is a normal distribution with mean intensity μ and standard deviation σ, U_i and V_i are assumed mutually independent.

2.2. The recovery algorithm

As an alternative to image sampling and acquisition problems we focus on utilizing dual sparse and redundant representations in the CS framework for fluorescence microscopic image denoising.

The proposed CS-based denoising scheme consists in determining the shorter exposition time X necessary to obtain, with a set of combined CS restorations associated to a set of sampling matrices Φ_i, a target SNR level, corresponding to the SNR measured on the image exposed T ms. This scheme provides the potential advantage of requiring a single shorter acquisition time, limiting degradation of the biological material through photo-damage and photo-bleaching. We also exploit the fact that fluorescence signal $\Phi_i x$ should be strongly correlated for all sampling matrix Φ_i, while noisy sampling $\Phi_i n$ should not be.

Combining CS reconstructions of a single noisy image acquisition $x + n$, using different sampling matrices Φ_i, is performed as described below:

$$\hat{x}_i = \arg \min_{x \in \mathbb{R}^N} \| \Psi x \|_{\ell_1} \text{ s.t. } \| y_i - \Phi_i x \|_{\ell_2} \leq \delta \quad (5)$$

for $i = 1...K$.

The last step of the algorithm involves the combination of $\hat{x}_i$ by averaging to generate a final denoised image $\hat{x}$. The number of images combined will introduce a regularization on the final image. We show that averaging grater number of images recovered with CS reduces exponentially the TV, as illustrated in Figure 1.
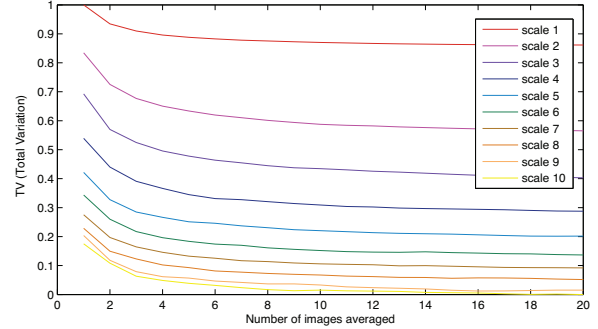

Fig. 1. TV versus number of images (Lymphocytes) recovered and combined for the 10 scales represented in Figure 2.
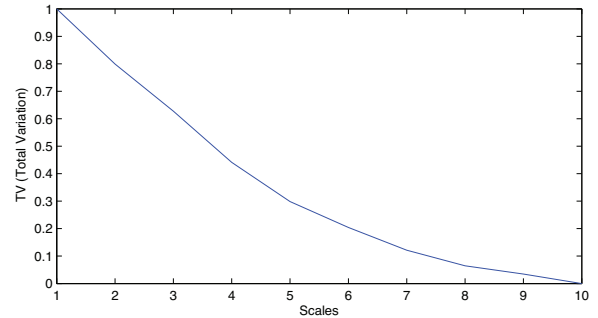

Fig. 2. TV versus scales for recovered images of Lymphocytes. Scales vary from a compression ratio exponentially increasing from $M = 30\%$ to $M = 0.3\%$.

3. CS AND SCALABILITY

With our working assumptions on the additive noise components, we propose to derive a series of CS reconstructions that will enable to separate noisy components from fluorescence signal reconstructions. The degree of freedom in this series of CS experiments in the choice of the sampling matrix Φ. Since the sparsity operator, TV, operates on the spatial domain, we chose to work with the orthogonal basis functions of random sampling in the Fourier domain. The degree of freedom for the choice of the Φ matrix, then becomes the number of random measurements M that is used. The CS theoretical framework states that the more measurements are used in the Φ domain, the closer is the reconstructed signal to the original measured signal. In the context of denoising (rather than estimation) we have a dual constraint on the noisy nature of the measurement and the risk to reconstruct these noisy components. Indeed, for a single CS experiment, the fluorescence signal will generate, from a set of random measures of structured Fourier values, a restored image with high values depicting a good estimation of the true signal. At the same time, purely random noisy component will be interpreted, from a set of undifferentiated Fourier values, as a structured combination of oscillating components, extrapolated over the spatial domain into patches, under the regularizing TV effect. Noise patches and fluorescence spatial localization will be directly related to M, the number of CS measurements acquired by Φ. We illustrate in Figure 3 and 4 how this number of measurements can be naturally viewed as a scale parameter, and in Figure 2 how the TV decrease beyond scales. For Figure 4, we cropped a background area from a fluorescence microscopic image, with pure noise signal, and performed CS reconstructions across scales (i.e. different numbers of
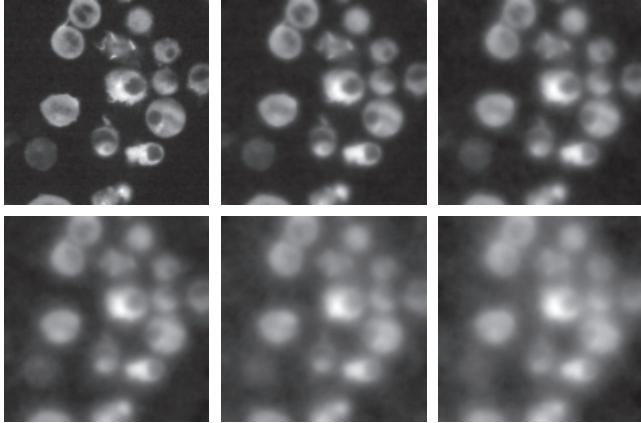
Fig. 3. Fluorescence microscopic image of Lymphocytes. Results from the same image recovered with six different numbers of measurements (i.e. 6 scales). Scales vary from a compression ratio exponentially increasing from $M = 30\%$ to $M = 0.3\%$.
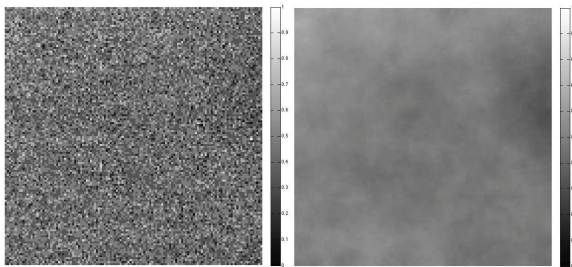

Fig. 5. Left: Pure noise image extracted from a microscopic image background. Right: Result obtained averaging 20 images recovered with different sets of measurements Φ_i for ($i = 1...20$).

measurements).

In the experiment on Figures 3 and 4, we observe that noise component is more uncorrelated than signal across scales while the spatial resolution of the signal component decreases. Increasing scale leads to a more difficult discrimination of signal and noise components.

We can make a connection here to the notion of multi-scale transforms which is discussed in [11]. These transforms were theoretically defined as linear transforms with a scale parameter controlling the ability of the transform to simplify the signal. We know from the sparsity constraint that strong true signals recovered by the CS framework will correspond to strong underlying components in the context of noise estimation from a small set of measurements. Therefore, CS does not introduce false signal components and fits well in the framework of multi-scale transforms, as illustrated in Figure 3.

Relaxing the constrain δ, which corresponds to the error allowed in (1), enables noise removal, or the appearance of patches which can present smooth edges. The difference between Figure 4 top and bottom comes from the relaxation of the constraint $\delta_{bottom} > \delta_{top}$, increasing smoothness of the reconstructed images. The good news is that in both cases, if results from CS reconstructions of a pure noise signal are combined at different scales, the mean intensity returns a nearly homogeneous signal, as seen in Figure 5. This observation clearly justifies the averaging operator introduced in section 2.2 to remove noise from images.
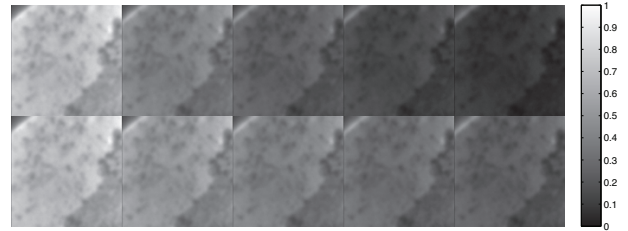

Fig. 6. Fluorescein images. Top: Six samples from the sequence of 200 images tagged with fluorescein. These images were acquired at $t = \{0, 500, 1000, 1500, 2000\}$ ms. Bottom: Supposed photobleaching resulted from 200 image acquisitions using CS denoising.

4. PHOTOBLEACHING

Photobleaching is a process in which fluorochrome molecules undergo photo-induced chemical destruction upon exposure to light excitation and loose their fluorescence ability. Benson et al. in [7] carried out an extensive study on the heterogeneous photobleaching rates, describing their experimental bleaching curve by a three-parameter exponential:

$$I_{(x,y,t)} = A_{(x,y)} + B_{(x,y)}e^{-kt} \qquad (6)$$

for each pixel in an image. Where $I_{(x,y,t)}$ is the fluorescence intensity at pixel (x, y) at time t, the offset $A_{(x,y)}$ is attributed to the background fluorescence, $B_{(x,y)}$ is the fluorescence intensity which decays exponentially and k is the rate of photon absorption (s^{-1}).

To verify the real photobleaching effect we have acquired 200 fluorescein images exposed 20 ms, with a negligible time transition between two consecutive image acquisitions, resulting in a total exposition time of 2000 ms. In this experiment we can clearly observe the fluorescence intensity decreasing exponentially as described by (6) and confirmed in the experience illustrated in Figure 6 and 8. As a consequence of the fluorescence intensity decreases, the SNR also decreases as show in Figure 7. Applying our CS-based method for denoising, we show that SNR can be highly improved while reducing photobleaching. Results on Figure 7 show that the rate between original SNR and CS-recovered images SNR is ~160%. Which means that still reaching an equivalent SNR, microscopic images could be acquired with a shorter exposition time, reducing photobleaching. The estimated final photobleaching improvement is illustrated in Figure 8 by the green curve, computed from the model described in Equation 6, fitting B and k values on the original images. Estimating the reduction of the exposition time necessary to achieve the same SNR as in the original data using the CS-based denoising scheme, we illustrate in Figure 8 with the green curve that photobleaching can be highly reduced. The same result can also be visualized in Figure 6.

5. CONCLUSION

In this paper we introduce a CS-based image acquisition and denoising method exploiting multiple reconstructions with random Fourier projections. Our approach presents several advantages over traditional denoising methods, joining image acquisition, CS advantages and denoising in one framework. Through some practical experiments, we have shown that our method can significantly improve the SNR on fluorescent microscopic images and that photobleaching can be highly reduced with shorter exposition times. Such results
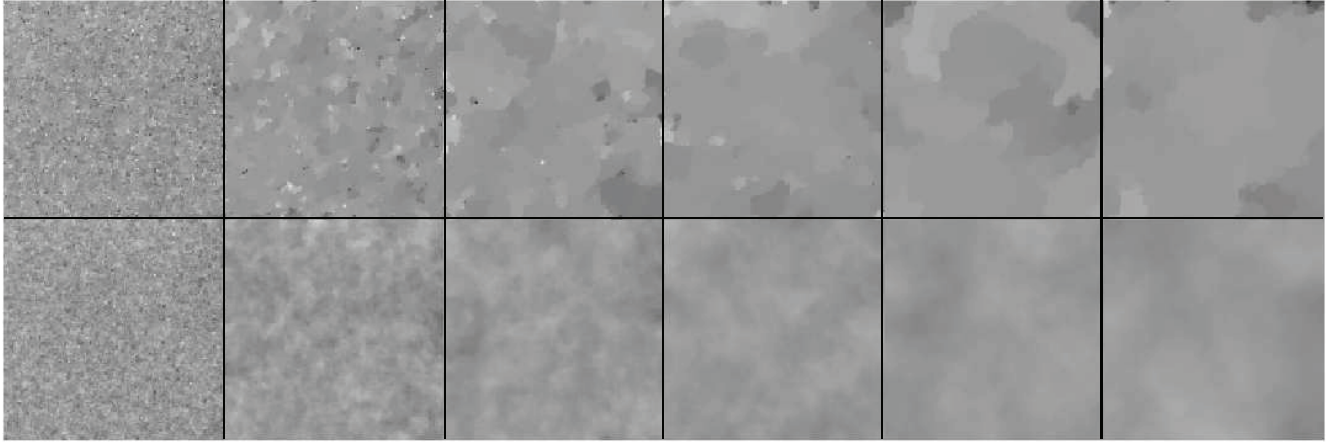
Fig. 4. Top: Pure noise signal extracted from a background patch of a microscopic image, recovered with six scales, (i.e. six different sizes of sample measurements). Scales vary exponentially from $M = 30\%$ to $M = 0.3\%$. Bottom: relaxing the constrain $\delta_{bottom} > \delta_{top}$.
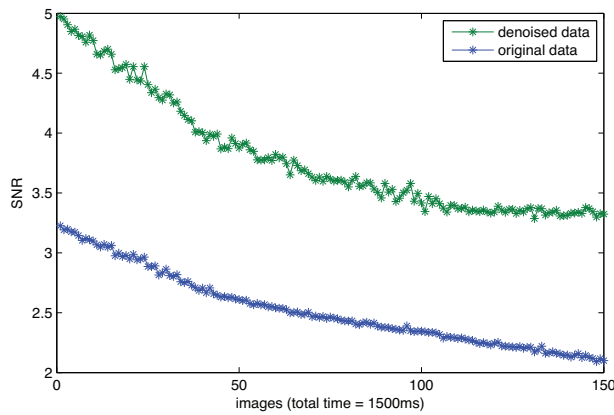

Fig. 7. SNR curves, we use a set of 150 fluorescein images acquired each $10\ ms$. The green line correspond to the SNR of images recovered with CS using the scheme proposed in Section 2.2 and the blue line correspond to the SNR of the original set of images.
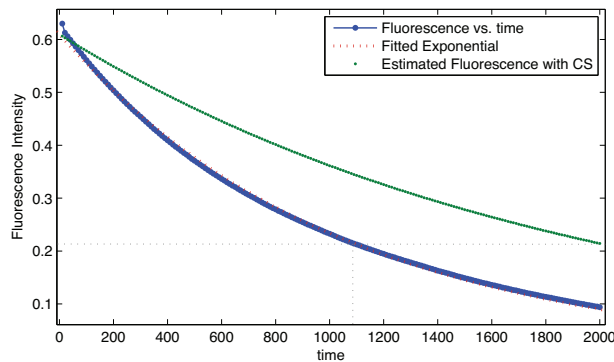

Fig. 8. Photobleaching curves, represented by the mean fluorescence intensity vs. time for original images of fluorescein (blue) and for images denoised with our proposed scheme (green). The red line corresponds to the exponential model fitted to the original data, setting specific values of B and k in Equation (6).

open the gate to new mathematical imaging protocols, offering the opportunity to reduce exposition time along with photo-damage and photo-bleaching and help biological applications based on fluorescence microscopy.

6. REFERENCES

[1] M. Lustig, D. Donoho, and J. M. Pauly, "Sparse MRI: The application of compressed sensing for rapid MR imaging," *Magnetic Resonance in Medicine*, vol. 58(6), pp. 1182–1195, December 2007.

[2] E. Candès, J. Romberg, and T. Tao, "Robust uncertainty principles: Exact signal reconstruction from highly incomplete frequency information," *IEEE Trans. on Information Theory*, vol. 52(2), pp. 489–509, June 2006.

[3] E. Candès, "Compressive sampling," in *Proceedings of the International Congress of Mathematics*, Madrid, Spain, 2006, vol. 3, pp. 1433–1452.

[4] E. Candès and J. Romberg, "Sparsity and incoherence in compressive sampling," *Inverse Problems*, vol. 23(3), pp. 969–985, November 2006.

[5] D. L. Donoho, "Compressed sensing," *IEEE Trans. on Information Theory*, vol. 52(4), pp. 1289–1306, April 2006.

[6] L. Song, E. J. Hennink, T. Young, and H. J. Tanke, "Photobleaching kinetics of fluorescein in quantitative fluorescence microscopy," *Biophysical Journal*, vol. 68, pp. 2588–2600, June 1995.

[7] D. M. Benson, J. Bryan, A. L. Plant, A. M. Gotto Jr., and L. C. Smith, "Digital imaging fluorescence microscopy: Spatial heterogeneity of photobleaching rate constants in individual cells," *THE JOURNAL OF CELL BIOLOGY*, vol. 100, pp. 1309–1323, April 1985.

[8] D. Donoho, M. Elad, and V. Temlyakov, "Stable recovery of sparse overcomplete representations in the presence of noise," *IEEE Transactions on Information Theory*, vol. 52, pp. 6–18, January 2006.

[9] E. Candès, J. Romberg, and T. Tao, "Stable signal recovery from incomplete and inaccurate measurements," *Communications on Pure and Applied Mathematics*, vol. 59(8), pp. 1207–1223, August 2006.

[10] E. Candès and J. Romberg, "Practical signal recovery from random projections," in *Proceedings of the SPIE Conference on Wavelet Applications in Signal and Image Processing XI*, San Jose, California, January 2005, p. 5914.

[11] T. Lindeberg, *Scale-Space Theory in Computer Vision*, The Kluwer International Series in Engineering and Computer Science, Dordrecht: Kluwer Academic, 1994.